Metrol. Meas. Syst., Vol. 30 (2023) No. 4, pp. 721–736
DOI: 10.24425/mms.2023.147958

PAN POLSKA AKADEMIA NAUK

METROLOGY AND MEASUREMENT SYSTEMS
Index 330930, ISSN 0860-8229
www.metrology.wat.edu.pl

M&MS

RECOGNIZING STEEL ELEMENTS WITH BRDF AND K-NEAREST NEIGHBORS

Adam Ciszkiewicz[1)], Janusz Jaglarz[2)], Tadeusz Uhl[3)]

1) Faculty of Mechanical Engineering, Cracow University of Technology, Al. Jana Pawła II 37, 31-864 Cracow, Poland (*pujaglar@cyfronet.pl*)
2) Faculty of Material Engineering, Cracow University of Technology, Al. Jana Pawła II 37, 31-864 Cracow, Poland (✉ *pujaglar@cyfronet.pl*)
3) Department of Robotics and Mechatronics, Faculty of Mechanical Engineering and Robotics, AGH University of Science and Technology, Al. Mickiewicza 30, 30-059, Cracow, Poland (*uhl@agh.edu.pl*)

Abstract

The paper deals with analysis of recognition of surface quality with reflective structures. Such surfaces are common in metallic materials cut using a saw or polished. There are no easy methods to identify such elements after machining. This issue is crucial in the industry for quality control as recognition of the elements, for instance after failure, allows for a detailed study of their manufacturing process. Firstly, six cuboid steel elements were obtained from a larger beam with a circular saw. Then, the bidirectional reflection distribution function (BRDF) was obtained for each element 3 times. The BRDF profiles were used in custom recognition software based on the K-nearest neighbors algorithm. In total, 140 variants of the classifier were tested and analyzed. Additionally, each variant was solved 200 times with different splits of the dataset. The results showed a high multiclass accuracy in all considered variants of the algorithm, with multiple variants achieving 100% accuracy. This level of performance was attained with only 1 to 2 training samples per class. Its low numerical complexity, easy experimental procedure, and "one-shot" nature allow for fast recognition, which is crucial in industrial applications.

Keywords: metallic surface, reflective surface, bidirectional reflection distribution function, classification.

1. Introduction

This paper discusses the possibilities of recognizing surfaces produced by periodic and semi periodic processes using *bidirectional reflection distribution function* (BRDF) scatterometry [1, 2] with a monochromatic (laser) light source. Surfaces with a topography resulting from the superposition of random and randomly periodic processes can be recognized with a *power spectral density* (PSD) frequency spectrum using the classification algorithms presented in this work. Research and analyzes performed to date have failed to provide reliable and unambiguous answers [3,4]. In other words, alternative optical measurement techniques are unreliable for highly

Article history: received May 5, 2023; revised July 31, 2023; accepted September 8, 2023; available online November 19, 2023.

reflective surfaces, especially when considering the time, simplicity and cost of the measurement. Papers or patents that would address the problem of fingerprinting for the recognition of large metallic surfaces are also missing from the literature.

Research on backscatter by surfaces is difficult to adapt to large-scale industrial research [5]. The large number of surfaces to be recognized in a short time negatively affects their reliability. Strong backscatter optical images obtained from *charge-coupled device* (CCD) cameras are characterized by low contrast, which greatly reduces the recognition accuracy of the engineering surface. Another problem is that each new surface is examined for production-related reasons at a slightly, but still, different angle of incidence. This results in decreased differentiation and increased unreliability of the recognition method.

In the methodology, the technique we propose for the recognition of highly reflective surfaces managed to avoid problems resulting from the change of measurement geometry, poor image contrast, and problems with the unreliability of recognition algorithms. For such engineering surfaces, a methodology based on the study of the Power Spectral Density determined by the BRDF method [6] proves the most efficient.

1.1. State of the art

Recognition of material surfaces has recently become an area of intense research to provide detailed information for applications such as autonomous agents and human-machine systems [7–9]. What is essential to recognizing different materials in images is modelling the apparent or latent characteristic appearance. Earlier research into modelling the appearance of materials largely focused on comprehensive laboratory measurements using dome systems, robots, or gonioreflectometers densely collecting measurements in angular space (such as BRDF or BTDF). This research, based on the reflectance factor, has the advantage of capturing the inherent surface properties in different variants, which enables the identification of fine-grained material [10].

The BRDF measurements provide an estimate of the reflectance factor, but only for diffuse scattering (hyperspectral cameras, *etc*.). Differential camera motion or object motion used for shape reconstruction were already used in early works [11]. However, the fundamental problem in surface recognition remains unsolved. Namely, we still do not know whether small changes in observation angles influence recognition performance.

Earlier publications demonstrated the effectiveness of angle filtering as a supplement to spatial filtering in material surface recognition. However, these methods rely on a mirror camera to capture a BRDF fragment [6] or a light camera [12,13] to obtain multiple differential variations and this requires specialized imaging equipment.

Texture recognition, 3D texture image classification, and bidirectional texture functions rely on projected 3D image functions and multiple views observed at different angles [13].

One of the methodologies used for materials surface recognition relies on modelling the detailed fundamental properties of the diffuse scattering of materials using the *bidirectional reflectance distribution function* (BRDF) and the *bidirectional transmittance distribution function* (BTDF) [1]. Material recognition is usually seen as a texture classification problem. Work on textiles directly address material recognition using multiple aligned images under different angles of view and lighting conditions.

The BRDF describes the appearance of a material through its interaction with light at a given surface point. Many analytical models represent the BRDF. However, these models are not commonly analyzed due to the lack of high-resolution measurement data. Due to the ease of

obtaining optical images, the BRDF is mostly used in measurements and models to render highly realistic computer graphics.

This paper presents a detailed study on how surface material recognition depends on light and observation conditions. There are studies in the literature [4, 5, 10–13] that cover BRDF models and new methods for the acquisition of angular spectra. In addition, interesting new BRDF-based methodologies keep emerging and they are used for rapid optical material recognition in industrial metrology, in particular, based on NIR spectroscopy image analysis [14, 15].

In terms of construction materials, most of the available studies focus on classifying and recognising defects on the surfaces of the elements. In this area, many different machine learning approaches have been employed, for instance: support vector machine [7, 8, 16], neural networks with attenuation mechanisms [17], convolutional neural networks [9, 18–23], classification priority networks [24], Siamese networks [25, 26], Siamese basis function networks [27], generative adversarial networks [28, 29], and k-nearest neighbors [30]. Furthermore, machine learning algorithms have also been used to recognize the phases of steel [31] and steel types [32–34] to model the mechanical properties of steel [35]. In general, approaches based on neural networks require significant datasets for training and validation, in most cases with additional annotation for supervised learning. This can be difficult and expensive to obtain. However, their advantage lies with their very broad capabilities in terms of classification. On the other hand, depending on the problem, simple methods such as k-nearest neighbors can work with smaller datasets, although their learning capabilities might be somewhat limited, when compared to the other methods.

On the other hand, the BRDF method has been proven effective in a variety of object recognition and classification problems [36]. It can be successfully employed to differentiate between alloys of the same material or different materials with only slight variations in texture [37, 38]. Some research groups have also studied optimal illumination for objects distinguishing [39]. Nevertheless, based on the performed literature search, BRDF has never been applied to recognize structural elements based on their normal surfaces after machining. Furthermore, most of the available classification methods have been applied to classify surface defects on steel and aluminum or to simply recognize the type of steel. To the best of our knowledge, there has not been a study yet, in which BRDF and a classification algorithm has been used to recognize a particular steel element's surface obtained by machining.

1.2. The aim of the study

This study aimed to propose and verify a novel method for recognition of steel elements surface based on BRDF and K-nearest neighbors [40]. Firstly, six cuboid steel elements were obtained from a larger beam using a circular saw. Then, the BRDF was obtained 3 times per element with remounting and at different heights. The BRDFs formed an initial dataset, which was split into training and testing portions. The train and test subsets were used to analyze 140 variants of the classifier. To minimize the effects of random number generation during dataset splitting, each variant was solved 200 times with different splits of the dataset. The performance of the classifier was measured using a multi-class accuracy measure.

The paper is organized in the following way. Section 1 presents the problem of metal surface recognition and identify the state of the art of analysis in the area of the presented research. The aim of the research is discussed. In Section 2, the methods proposed by the authors are shown, experiment results are discussed and used for validation of the formulated method of metal surface classification. Section 3 presents the results of steel surface classifications and discusses their quality. Section 4 includes conclusions and final remarks.

2. Materials and methods

2.1. The experiment

Firstly, a rectangular steel beam was cut into six cuboid elements with a circular saw for cutting steel (see Fig. 1a). The surfaces of the obtained elements were visually indistinguishable (see Fig. 1b). Then, BRDF was registered 3 times for each element (18 BRDFs in total). Each measurement was performed at a different height, with element remounting (see Fig. 1c).

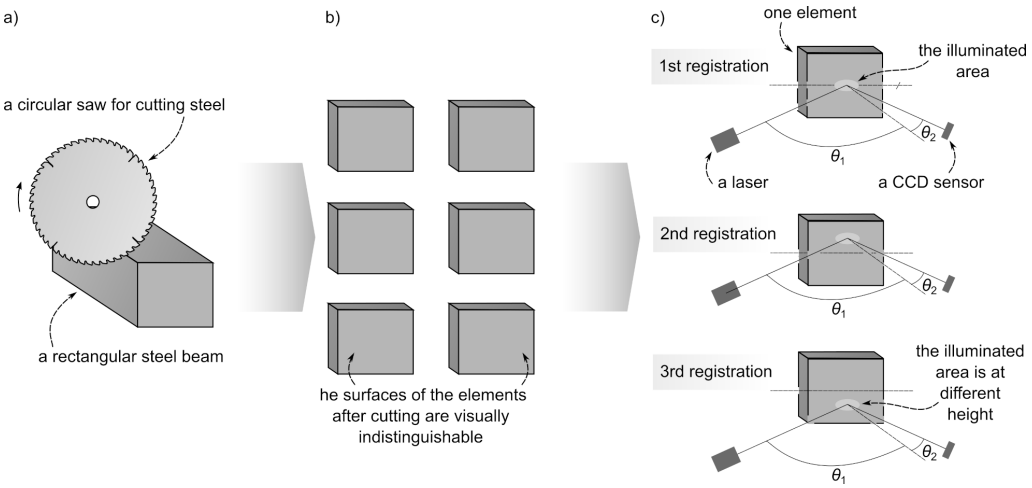

Fig. 1. Overview of the experiment: a) a steel beam cut into smaller elements, b) the six elements with indistinguishable normal surfaces, c) the BRDF registration (3× per element), where: θ_1 – the incidence light angle, θ_2 – outgoing light angle.

In the BRDF measurement, the tested steel cuboids were illuminated with a light source – laser diode 635. The light reflected from the element was registered using a high-sensitivity Si detector [41]. Both the light source and the detector were mounted on a goniometric table, which allowed the user to change the incidence/scattering light angle and the orientation of the sample.

In the most general form, the BRDF function depends on four variables: incidence light angle θ_1, outgoing light angle θ_2, and two angles defining the orientation of the element with regard to the light source. The full BRDF functions are usually obtained for light-response models used in computer graphics. As it is a time-consuming experiment, recording of the complete light response is not viable in an industrial setting. Hence, in this study a constant incidence light angle $\theta_1 = 60.00$ deg (see Fig. 1c) and constant orientation were assumed. The latter is justifiable in industrial applications – typical products often have distinct geometrical shapes with at least one flat surface. This flat surface can be used to orient the elements with regard to the light source. The only variable angle in the procedure was the outgoing light angle varied from $\theta_{2\,\mathrm{min}} = 70.00$ deg to $\theta_{2\,\mathrm{max}} = 83.75$ deg, with $\Delta\theta_2 = 0.05$ deg. This range was limited by the capabilities of the measurement equipment.

In this case, the BRDF measured the differential of the scattered beam power per the solid angle of the receiver aperture $\mathrm{d}P/\mathrm{d}\Omega$ (in the θ_2 direction) divided by incident power P_1 in the direction θ_1. The differential $\mathrm{d}P/\mathrm{d}\Omega$ can be expressed as the ratio of measured scatter power P_2

and detector acceptance angle Ω [6]:

$$\mathrm{BRDF} = \frac{\mathrm{d}P/\mathrm{d}\Omega}{P_1 \cos\theta_2} = \frac{P_2}{P_1 \Omega \cos\theta} \,. \tag{1}$$

Furthermore, the domain of the obtained BRDFs was converted to spatial frequency f using the following formula [6]:

$$f = \left(\sin\theta_2 - \sin\theta_1\right)/\lambda \,, \tag{2}$$

where: θ_2 – the scattering light angle (here: $\theta_2 \in \langle 70.00 \text{ deg}; 83.75 \text{ deg}\rangle$), θ_1 – the incidence light angle (here: $\theta_1 = 60$ deg), λ – the wavelength of the laser (here: $\lambda = 635$ nm).

2.2. Algorithms – metal surfaces classification

The main aim of this study was to propose and verify a method for recognizing steel elements based on their unique cross-sections created by a circular saw. The task of recognizing particular elements can be defined as a classification problem – a supervised machine learning problem. In this case, a set of training samples with their corresponding classes is given to the classification algorithm. The algorithm learns characteristic features from the training samples and can be used to predict the class of previously unseen samples. The performance of such an algorithm can be measured by predicting a class of multiple unseen samples, for which the actual class is known. In practice, this is often done by splitting the original dataset into two subsets: training and testing sets – only the training part is used for teaching the algorithm, while the test part is applied to assess its predictive capabilities. In the context of steel element recognition, the classes correspond to the IDs of the steel elements, while the samples are the registered BRDF signals. The main task is to assign an element ID (class) to an unknown BRDF signal (sample) using an algorithm trained on a set of BRDFs, for which the IDs are known. Given the lengthy process of BRDF acquisition and the possible industrial application of the procedure, the number of training samples should be as low as possible – preferably: one per class, which is often referred to as "one-shot" [26, 27, 42].

2.2.1. The classification algorithm

In this study, the classification procedure was based on the *K-nearest neighbors* algorithm (KNN) [40], with $K = 1$, which is a common approach in machine learning [43, 44]. The working principle of the method is very simple – given an unknown signal, the algorithm iterates over all training signals and compares them to the unknown signal. The comparison is carried out with the Minkowski distance, a common metric [45], which for one-dimensional BRDF signals can be written as follows:

$$\left\|\mathrm{BRDF}_i - \mathrm{BRDF}_j\right\| = \sqrt[p]{\sum_{k=1}^{n} \left|\mathrm{BRDF}_i(f_k) - \mathrm{BRDF}_j(f_k)\right|^p} \,, \tag{3}$$

where: $\mathrm{BRDF}_i(f_k)$ – the value of the registered BRDF signal is i at the spatial frequency f_k, n – the number of BRDF samples, p – the order of the Minkowski distance – in this study $p = 1$ and $p = 2$ were used, which are commonly referred to as the Manhattan and Euclidean distance. Notably, the Manhattan distance is less expensive to compute than the Euclidean one [46], while the Euclidean metric is a more natural way to specify a distance.

After the comparison, the training signal with the lowest distance (3) is selected and the class of this signal is assigned to the unknown sample. The basic procedure for classifying one unknown sample from the test set was presented in Fig. 2.

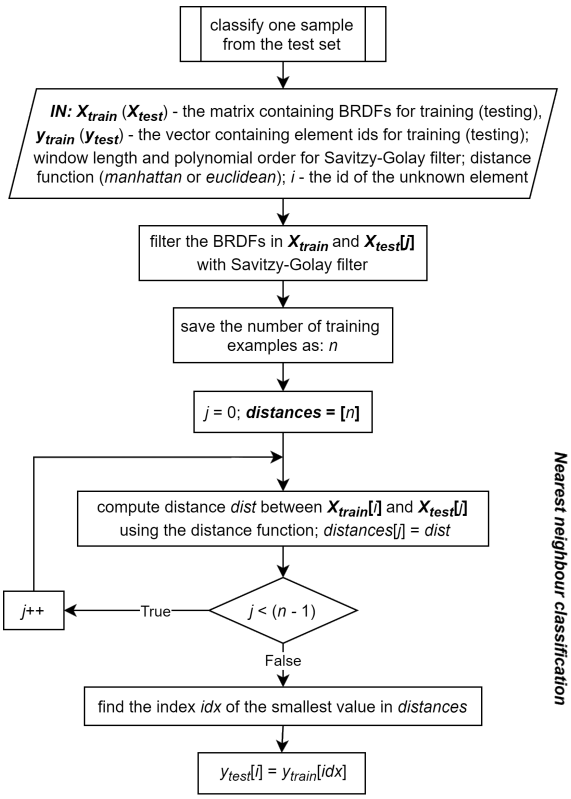

Fig. 2. The flowchart presenting the procedure used to classify one unknown sample from the test set based on the given train set and train classes.

2.2.2. Signal pre-processing

The KNN classifier can be used with raw BRDF signals, nevertheless, such signals are prone to various sources of noise, which can impact the predictive capabilities of the model. Therefore, in this study, we decided to apply additional filtration on all registered BRDF signals – as seen in Fig. 2. The filtration was carried out with a Savitzky-Golay filter [47]. It is worth mentioning that this could be done with many other methods, including other convolution-based filters, such as a median filter or a Gaussian filter. The primary reason for choosing the Savitzky-Golay was its ability to suppress the noise, while preserving signal peaks [48], which could correspond to the characteristic marks left on the surface by the machining.

This digital filter was used to fit low-order polynomials to subsets of the original signal. The two main parameters of the filter were the order of the polynomial (here: from 2 to 10) and the window length (here: from 11 to 271 with a step of 20). Higher polynomial orders were not explored as the quality of results degraded due to numerical issues. Additionally, it was possible to specify the behavior of the filter near the edges of the signal – in this study, the signal was mirrored. The filter was incorporated into the classifier using a *Python* library – *Scipy* [49] (*scipy.signal.savgol_filter*). The effects of different parameters of the Savitzky-Golay filter on a sample BRDF signal were presented in Fig. 3. In general, if we increase the length of the window and decrease the order of the polynomial, we obtain a more smoothed filtered signal.

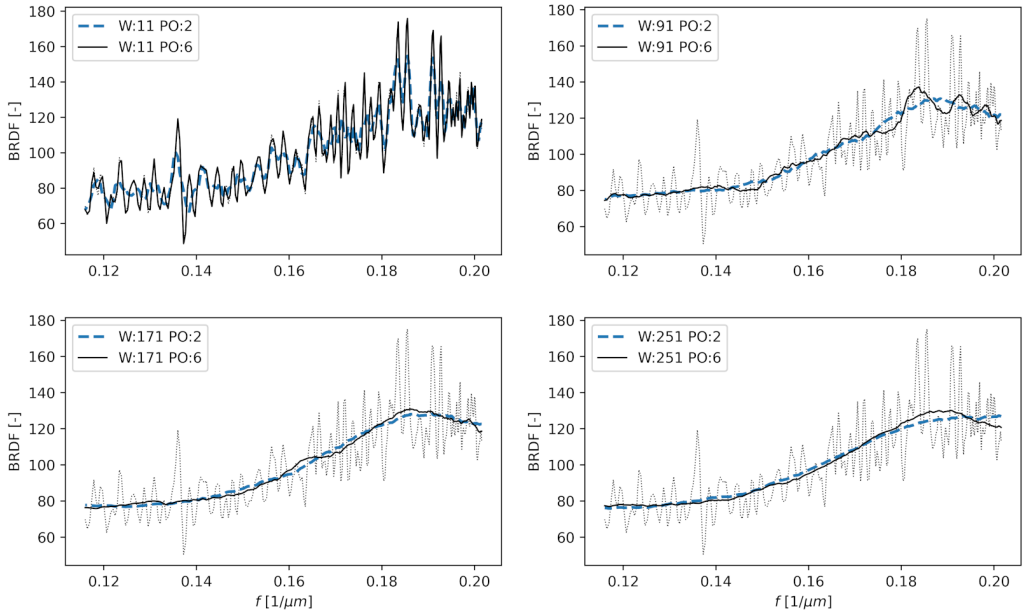

Fig. 3. Effects of different parameters of the Savitzky-Golay filter on a sample BRDF signal over signal with very low filtration (dotted line), where: W – window length, PO – polynomial order.

2.2.3. Analysis of the prediction quality

Since the best values for the parameters of the Savitzky-Golay filter were difficult to find and the choice of the distance metric was not obvious, we decided to check different variations of the classifier. Namely, 14 values of window length (from 11 to 271 with a step of 20), 9 orders of polynomials (from 2 to 10), and 2 types of distance (Manhattan and Euclidean – see (3)) were considered in this study. These parameters were analyzed in a grid-like fashion, which resulted in 252 ($14 \cdot 9 \cdot 2$) variants of the algorithm.

As mentioned before, the experiment results consisted of 3 repetitions of BRDF per element. In total, the dataset contained 18 BRDF samples over 6 classes. To test the predictive capabilities of the classifier, the original dataset was divided into the train and test subsets. The assignment of samples was random, nevertheless, each of the subsets had to have at least one sample from each class – in other words, all classes had to be represented in both subsets, which meant a subset had between 6 and 12 samples. The dataset splitting procedure was performed 200 times per classifier variant to minimize the effects of random number generation. In total, the classifier testing procedure was executed 50400 times, which was the 252 variants of the algorithm (see the previous paragraph) tested on 200 shuffles of the dataset to minimize the effects of the random number generator.

The quality of prediction for each variant was measured using a multiclass accuracy metric [43], computed with the following formula for each run:

$$\mathrm{acc}_j = \frac{1}{k} \sum_{i=1}^{k} \frac{m_{c,i}}{m_i}, \tag{4}$$

where: acc_j – the multiclass accuracy metric [43] in run j (where $j < 200$), $m_{c,i}$ – number of correct predictions of class i in the test set; m_i – number of occurrences of class i in the test set, k – number of classes.

As mentioned before, each classifier (*i.e.* variant of the algorithm) was assessed 200 times on different shuffles of the dataset using (4) for computing accuracy. The final score for each of the variants was the average accuracy over 200 runs computed as follows:

$$\mathrm{acc} = \frac{1}{200}\sum_{j=0}^{200}\mathrm{acc}_j\,, \tag{5}$$

where: acc – the final accuracy score obtained by the variant of the classifier, acc_j – the multiclass accuracy metric [43] in run j (where $j < 200$).

3. Results and discussion

The results section is divided into three subsections. The first one presents the obtained BRDF profiles, while the second one is focused on the performance of the proposed classification procedure. The third one discusses the sensitivity of the procedure with regard to the signal filtration method.

3.1. The obtained BRDF profiles

The obtained BRDF profiles are presented in Fig. 4. The shapes of these curves for all elements are unique – see Fig. 4a. The signals overlap for spatial frequencies higher than 0.14 1/µm making

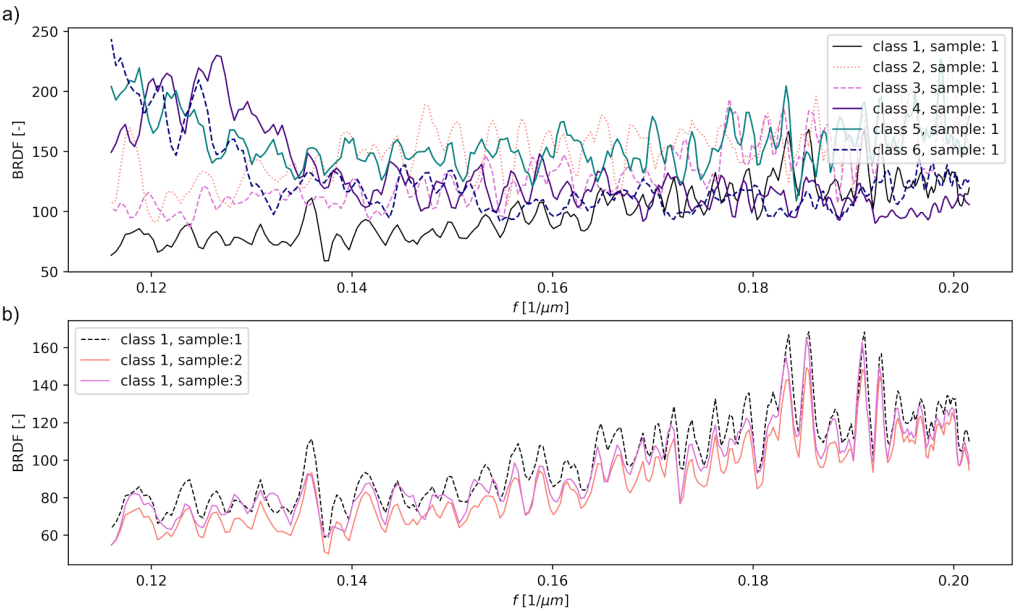

Fig. 4. BRDF profiles over spatial frequency f after filtration with the Savitzky-Golay a) window length: 7, polynomial order: 2, mode: mirrored and one BRDF per element; b) three BRDFs for element 1.

them difficult to distinguish visually. Furthermore, it is worth noting that this part of the figure contains only one sample per element. The differences between the BRDFs registered for one element with remounting can also be significant as seen in Fig. 4b.

3.2. The performance of the classifier

In total, 44 variants of the algorithm achieved perfect accuracy of 100.00% over 200 runs with different train/test splits. Selected ones were detailed in Table 1. This was done using a moderate level of filtration with a window length from 47 to 87 and a polynomial order from 4 to 6. Interestingly, within the best variants, the Euclidean distance measure was employed in 35 out of 44 cases. This showcased its suitability to the studied problem. It is worth mentioning that the classifiers with filtration significantly outperformed the baseline – the classifiers without filtration – which, in the best case, achieved a mean accuracy of 98.71%.

Table 1. The multiclass accuracy for the five best and worst variants of the classifier along with their parameters, mean accuracy of the 252 variants, and baseline accuracy obtained for the classifier with no filtration applied to BRDFs, where "*Avg acc*" means accuracy averaged over the final scores of 252 variants.

Best acc [%]	**Distance**	**Window length**	**Polynomial order**
100.00	Euclidean	71	4
100.00	Euclidean	51	10
100.00	Euclidean	51	8
100.00	Euclidean	51	7
100.00	Euclidean	51	6
Worst acc [%]	**Distance**	**Window length**	**Polynomial order**
89.62	Manhattan	271	3
90.00	Manhattan	251	3
90.33	Manhattan	271	2
90.46	Manhattan	211	2
90.50	Manhattan	211	10
Avg acc [%]			
97.43	–	–	–
acc with no filtration [%]			
98.71	Euclidean	–	–
98.46	Manhattan	–	–

Significantly worse results were obtained with highly filtered signals, which meant a large window length and a low polynomial order. The worst variant achieved an accuracy of only 89.62%. Furthermore, all of the five worst cases were obtained using the Manhattan distance metric. The overall average accuracy of the 252 variants was 97.43%.

Based on these findings, it can be seen that moderate filtration was beneficial to the prediction accuracy, while overfiltration resulted in unsatisfactory performance of the algorithm. This might suggest that high-frequency information in BRDFs is essential for recognition of steel-based elements. Nonetheless, it has to be pointed out that even in the worst-case scenario, the classifier still achieved nearly 90% accuracy, which is a good result when predicting 6 classes.

The conclusions drawn from Table 1 were further exemplified using a contour plot of accuracy with regard to polynomial order and window length, presented in Fig. 5. Both very low and very high filtration levels resulted in suboptimal performance of the classifier. The issue was especially evident for high values of the window length combined with low polynomial order. Very good accuracy was achieved under moderate filtration levels – window length between 31 and 91. It is worth mentioning that predictions were also valid with higher values of the window length (> 91), but with a high order of the polynomial. This could be explained by the fact that higher-order polynomials have greater flexibility in terms of following the signal, and the filtered signal retains more high-frequency details – refer to Fig. 3 for a visual example. Nevertheless, it is worth mentioning that higher polynomial orders offer clear benefits only to the 9th order. After that, the general performance of the classifier drops, likely due to numerical issues with higher order polynomials. Again, these findings suggested that the information differentiating the signals was in the high-frequency part of the BRDFs.

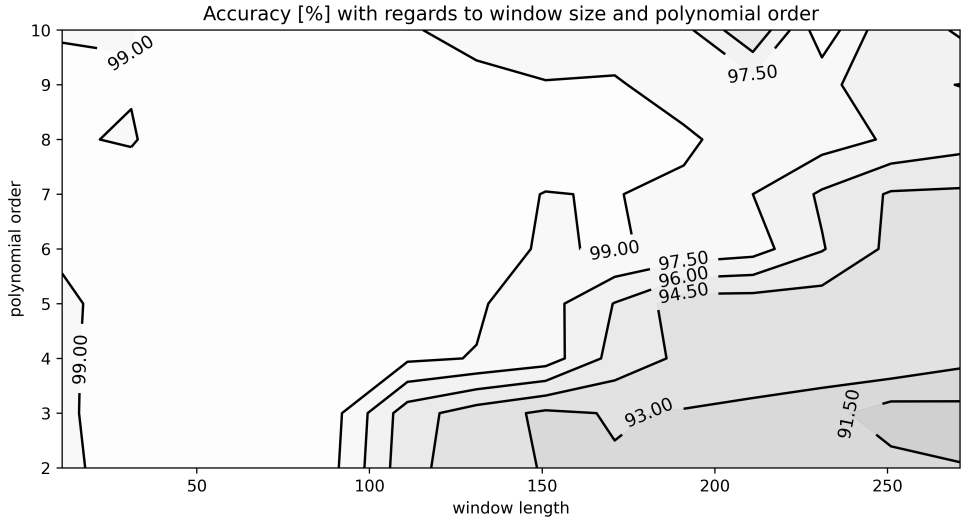

Fig. 5. Contour plot presenting the accuracy (acc) of the classifier with regard to the window length and polynomial order of the Savitzky-Golay filter applied to BRDF signals.

In terms of the distance metric, the Euclidean approach offered better results both in the average as well as the worst case, as seen in Table 2. Nonetheless, both metrics were capable of achieving perfect performance on the test set with 100.00% accuracy, assuming proper levels of filtration (here: window length of 51 and polynomial order of 6 or 7).

Note that our approach achieved this level of performance with only 1 or 2 training samples per class. This “one-shot” nature of the approach is an important characteristic and might make the method an interesting choice for large-scale industrial applications. Nevertheless, it should be noted that our original dataset had only 18 samples. More samples could showcase some outliers, for instance due to different external conditions, equipment limitations or measurement problems. Furthermore, the range of the spatial frequencies might also be minimized to shorten the experiment. Therefore, in a future study, this analysis should be carried out on a larger dataset with more classes and samples per class.

Metrol. Meas. Syst., Vol. 30 (2023), No. 4, pp. 721–736
DOI: 10.24425/mms.2023.147958

Table 2. The best, worst, and mean multiclass accuracy for the classifier when using the Euclidean and Manhattan distance, where "*Avg acc*" means accuracy averaged over the final accuracy scores of 126 variants with the Euclidean/Manhattan distance.

Euclidean			**Window length**	**Polynomial order**
	Avg acc [%]	97.94	–	–
	Best acc [%]	100.00	51	6
	Worst acc [%]	91.46	251	3
Manhattan				
	Avg acc [%]	96.92	–	–
	Best acc [%]	100.00	51	7
	Worst acc [%]	89.62	271	3

3.3. The sensitivity of the classifier with regard to the filtration method

As mentioned in Section 2.2.3, there were many available approaches for signal filtration. The Savitzky-Golay method was just one of the available options. It was selected because of its ability to filter the noise, while preserving peaks in the signal [48], which could correspond to the marks caused by machining on the surface of the elements. Nevertheless, to critically assess this choice, we decided to test the Savitzky-Golay against some other popular choices in signal filtration – the median filter and the Gaussian filter.

The median filter was directly compared to the Savitzky-Golay as it featured the same parameter – window length. The results were presented in Fig. 6. In this case, the peak-preserving ability of the Savitzky-Golay filter was clear and, for larger windows, the proposed approach was better. It should also be mentioned that the median filter was capable of achieving 100% accuracy for very small window lengths. In these cases, only some of the noise was filtered, but high frequency information was still retained.

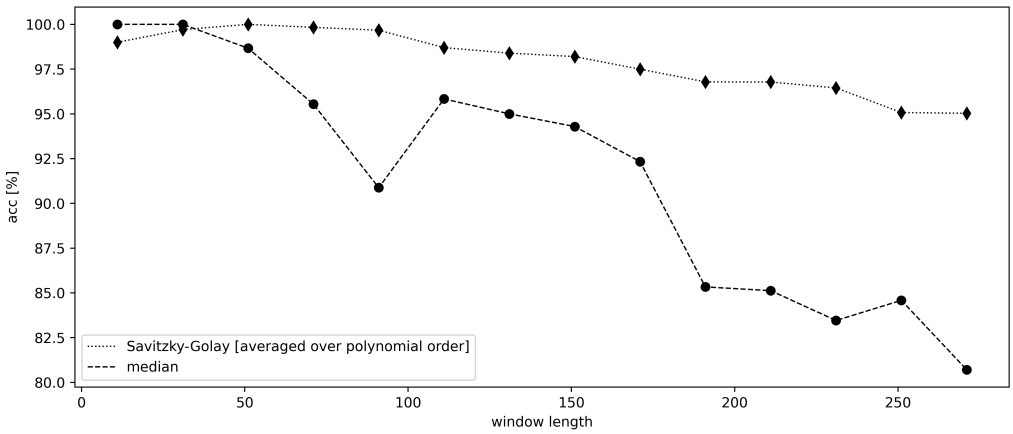

Fig. 6. Plot presenting the accuracy (acc) of the classifier with the Savitzky-Golay filter against the median filter with regard to the used window length. In both cases the algorithm's Euclidean distance was used. The results from the Savitzky-Golay were averaged over the polynomial order from 2 to 10.

With Gaussian filtration it was more difficult to directly compare the results, as the Gaussian filter used standard deviation as its main parameter. Nevertheless, we have found that for relatively small standard deviations (from 1.0 to 5.0) the Gaussian filter could also achieve 100% accuracy with the Euclidean distance – see Fig. 7. We have concluded that this meant that our assumption to employ BRDF to differentiate steel elements was correct. Nevertheless, larger values of standard deviation degraded the results significantly, as the signal peaks were no longer preserved. In comparison, the Savitzky-Golay filter was much more stable when tested over a wide range of its parameters. We believe that this feature might be even more pronounced with larger datasets.

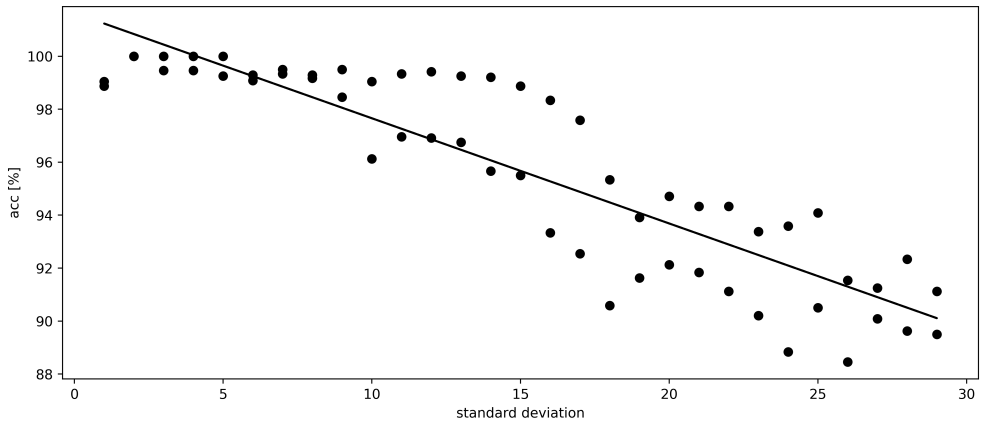

Fig. 7. Plot presenting the accuracy (acc) of the classifiers with a Gaussian filter with regard to its standard deviation (*sigma*). Two points per standard deviation correspond to Euclidean and Manhattan distance metrics. The solid line represents is the linear regression over the obtained results, which showcases degrading performance with higher standard deviation.

4. Conclusions and final remarks

1. In this study, a novel method for the recognition of surface features of steel elements was presented. The procedure was based on BRDF and KNN with Savitzky-Golay filtration. To verify the procedure, a set of 18 BRDFs were acquired from 6 cuboid steel elements. In total, 252 variants of the classifier were tested and analyzed with the original dataset split into training and testing portions. To minimize the effects of random number generation, each variant was solved 200 times with different splits of the dataset.
2. The obtained results showed that the proposed approach offers a very high multiclass accuracy in all the considered variants of the algorithm. Furthermore, multiple variations achieved a perfect accuracy score of 100% using moderate filtration.
3. It should be noted that this level of performance was attained using only 1 or 2 training samples per class. While it is true that the current performance is satisfactory even with 1 or 2 training samples per class, more samples might showcase some outliers. Furthermore, the range of the spatial frequencies might be minimized to shorten the experiment. Therefore, in the future an extended study should be performed on a larger dataset.
4. Very high levels of signal filtration were found to lower the accuracy score of the classificator. Similarly, signals with very low level of filtration contained too much high-frequency noise for classification. Best results were obtained under moderate filtration, which meant the polynomial order between 4–9 and window size close to 51.

5. To summarize, the method offered great predictive capabilities, while being both non-destructive and easy to implement. Additionally, its low numerical complexity, easy experimental procedure, and "one-shot" nature allow for fast recognition, which is crucial in industrial use. It is our belief that the method could be extended to machined elements made from different materials. Future work will be focused on testing the method in large-scale industrial applications and extending the approach to elements with curved geometry. Furthermore, we also plan to increase the illuminated area, which could improve the recognition results as more surface features would be registered.

References

[1] Nicodemus, F. E. (1965). Reflectance Nomenclature and Directional Reflectance and Emissivity. *Applied Optics*, *4*(7), 767–775. https://doi.org/10.1364/ao.9.001474

[2] Asmail, C. (1991). Bidirectional scattering distribution function (BSDF): A systematized bibliography. *Journal of Research of the National Institute of Standards and Technology*, *96*(2), 215–223. https://doi.org/10.6028/jres.096.010

[3] Neogi, N., Mohanta, D. K., & Dutta, P. K. (2014). Review of vision-based steel surface inspection systems. *EURASIP Journal on Image and Video Processing*, *50*. https://doi.org/10.1186/1687-5281-2014-50

[4] Mikeš, S., & Haindl, M. (2019). View Dependent Surface Material Recognition. Bebis G. *et al.* (Eds) *Advances in Visual Computing. ISVC 2019. Lecture Notes in Computer Science*, *11844*. Springer, Cham.

[5] Hahlweg, C., & Rothe, H. (2005). Classification of optical surface properties and material recognition using multi-spectral BRDF data measured with a semi-hemispherical spectro-radiometer in VIS and NIR. *Proc. SPIE 5965, Optical Fabrication, Testing, and Metrology II, 59650G*. https://doi.org/10.1117/12.624838

[6] Stover, J. C. (1995). *Optical Scattering: Measurement and Analysis (2nd. ed.)*. SPIE Press. https://doi.org/9780819478443

[7] Gong, R., Wu, C., & Chu, M. (2018). Steel surface defect classification using multiple hyper-spheres support vector machine with additional information. *Chemometrics and Intelligent Laboratory Systems*, *172* (December 2017), 109–117. https://doi.org/10.1016/j.chemolab.2017.11.018

[8] Chu, M., Gong, R., Gao, S., & Zhao, J. (2017). Steel surface defects recognition based on multi-type statistical features and enhanced twin support vector machine. *Chemometrics and Intelligent Laboratory Systems*, *171* (August), 140–150. https://doi.org/10.1016/j.chemolab.2017.10.020

[9] Zheng, X., Wang, H., Chen, J., Kong, Y., & Zheng, S. (2020). A Generic Semi-Supervised Deep Learning-Based Approach for Automated Surface Inspection. *IEEE Access*, *8*, 114088–114099. https://doi.org/10.1109/ACCESS.2020.3003588

[10] Rakels, J. H. (1989). Recognised Surface Finish Parameters Obtained from Diffraction Patterns of Rough Surfaces. *Proc. SPIE 1009, Surface Measurement and Characterization*.

[11] Kumar, H., Ramkumar, J., & Venkatesh, K. S. (2018). Surface texture evaluation using 3D reconstruction from images by parametric anisotropic BRDF. *Measurement: Journal of the International Measurement Confederation*, *125* (April), 612–633. https://doi.org/10.1016/j.measurement.2018.04.090

[12] Ngan, A., Durand, F., & Matusik, W. (2005). Experimental Analysis of BRDF Models. *Mitsubishi Electric Research Laboratories*

[13] Ghosh, A., Achutha, S., Heidrich, W., & O'Toole, M. (2007). BRDF acquisition with basis illumination. 2007 *IEEE 11th International Conference on Computer Vision* (pp. 1-8). IEEE. https://doi.org/10.1109/ICCV.2007.4408935

[14] Dana, K. J. (2001). BRDF/BTF Measurement Device. *Proceedings Eighth IEEE International Conference on Computer Vision*, *ICCV 2001* (Vol. 2, pp. 460–466). IEEE. https://doi.org/10.1109/ICCV.2001.937661

[15] Lai, Q., Liu, B., Zhao, J., Zhao, Z., & Tan, J. (2020). BRDF characteristics of different textured fabrics in visible and near-infrared band. *Optics Express*, *28*(3), 3561. https://doi.org/10.1364/oe.385135

[16] Liu, Y., Xu, K., & Xu, J. (2019). An improved MB-LBP defect recognition approach for the surface of steel plates. *Applied Sciences (Switzerland)*, 9(20). https://doi.org/10.3390/app9204222

[17] Zhang, D., Song, K., Xu, J., He, Y., & Yan, Y. (2020). Unified detection method of aluminium profile surface defects: Common and rare defect categories. *Optics and Lasers in Engineering*, *126* (August 2019). https://doi.org/10.1016/j.optlaseng.2019.105936

[18] Acharya, A. K., Sahu, P. K., & Jena, S. R. (2019). Deep neural network based approach for detection of defective solar cell. *Materials Today: Proceedings*, *39*, 2009–2014. https://doi.org/10.1016/j.matpr.2020.09.048

[19] Gao, Y., Gao, L., Li, X., & Yan, X. (2020). A semi-supervised convolutional neural network-based method for steel surface defect recognition. *Robotics and Computer-Integrated Manufacturing*, *61* (May 2019). https://doi.org/10.1016/j.rcim.2019.101825

[20] Chen, W., Gao, Y., Gao, L., & Li, X. (2018). A New Ensemble Approach based on Deep Convolutional Neural Networks for Steel Surface Defect classification. *Procedia CIRP*, 72, 1069–1072. https://doi.org/10.1016/j.procir.2018.03.264

[21] Fu, G., Sun, P., Zhu, W., Yang, J., Cao, Y., Yang, M. Y., & Cao, Y. (2019). A deep-learning-based approach for fast and robust steel surface defects classification. *Optics and Lasers in Engineering*, *121* (February), 397–405. https://doi.org/10.1016/j.optlaseng.2019.05.005

[22] Kou, X., Liu, S., Cheng, K., & Qian, Y. (2021). Development of a YOLO-V3-based model for detecting defects on steel strip surface. *Measurement*, 109454. https://doi.org/10.1016/j.measurement.2021.109454

[23] He, X., Wang, T., Wu, K., & Liu, H. (2021). Automatic defects detection and classification of low carbon steel WAAM products using improved remanence/magneto-optical imaging and cost-sensitive convolutional neural network. *Measurement*, 173 (August 2020), 108633. https://doi.org/10.1016/j.measurement.2020.108633

[24] He, D., Xu, K., & Zhou, P. (2019). Defect detection of hot rolled steels with a new object detection framework called classification priority network. *Computers and Industrial Engineering*, 128 (December 2018), 290–297. https://doi.org/10.1016/j.cie.2018.12.043

[25] Kim, M. S., Park, T., & Park, P. (2019). Classification of Steel Surface Defect Using Convolutional Neural Network with Few Images. *2019 12th Asian Control Conference*, *ASCC 2019* (pp. 1398–1401).

[26] Deshpande, A. M., Minai, A. A., & Kumar, M. (2020). *One-shot recognition of manufacturing defects in steel surfaces*. *Procedia Manufacturing*, *48*, 1064–1071. https://doi.org/10.1016/j.promfg.2020.05.146

[27] Schlagenhauf, T., Yildirim, F., Brückner, B., & Fleischer, J. (2020). Siamese basis function networks for defect classification. ArXiv.

[28] Di, H., Ke, X., Peng, Z., & Dongdong, Z. (2019). Surface defect classification of steels with a new semi-supervised learning method. *Optics and Lasers in Engineering*, *117* (February), 40–48. https://doi.org/10.1016/j.optlaseng.2019.01.011

[29] He, Y., Song, K., Dong, H., & Yan, Y. (2019). Semi-supervised defect classification of steel surface based on multi-training and generative adversarial network. *Optics and Lasers in Engineering*, *122*(May), 294–302. https://doi.org/10.1016/j.optlaseng.2019.06.020

[30] Nguyen, V. H., Pham, V. H., Cui, X., Ma, M., & Kim, H. (2017). Design and evaluation of features and classifiers for OLED panel defect recognition in machine vision. *Journal of Information and Telecommunication*, *1*(4), 334–350. https://doi.org/10.1080/24751839.2017.1355717

[31] Gupta, S., Sarkar, J., Kundu, M., Bandyopadhyay, N. R., & Ganguly, S. (2020). Automatic recognition of SEM microstructure and phases of steel using LBP and random decision forest operator. *Measurement*, *151*, 107224. https://doi.org/10.1016/j.measurement.2019.107224

[32] Ciocan, R., Petulescu, P., Ciobanu, D., & Roth, D. J. (2000). Use of the neural networks in the recognition of the austenitic steel types. *NDT and E International*, *33*(2), 85–89. https://doi.org/10.1016/S0963-8695(99)00032-8

[33] Arenas, M. P., Rocha, T. J., Angani, C. S., Ribeiro, A. L., Ramos, H. G., Eckstein, C. B., Rebello, J. M. A., & Pereira, G. R. (2018). Novel austenitic steel ageing classification method using eddy current testing and a support vector machine. *Measurement*, *127* (September 2017), 98–103. https://doi.org/10.1016/j.measurement.2018.05.101

[34] Zhang, T., Xia, D., Tang, H., Yang, X., & Li, H. (2016). Classification of steel samples by laser-induced breakdown spectroscopy and random forest. *Chemometrics and Intelligent Laboratory Systems*, *157*, 196–201. https://doi.org/10.1016/j.chemolab.2016.07.001

[35] Khudhair, S., Taher, M. K., & Mohammed, M. (2021). Strain rate effect on mechanical properties of 0.24% carbon steel using artificial neural network. *Materials Today: Proceedings*, https://doi.org/10.1016/j.matpr.2021.03.514

[36] Shiradkar, R., Shen, L., Landon, G., Ong, S. H., & Tan, P. (2014). A new perspective on material classification and ink identification. *Proceedings of the IEEE Computer Society Conference on Computer Vision and Pattern Recognition* (pp. 2275–2282). https://doi.org/10.1109/CVPR.2014.291

[37] Liu, C., Yang, G., & Gu, J. (2013). Learning discriminative illumination and filters for raw material classification with optimal projections of bidirectional texture functions. *Proceedings of the IEEE Computer Society Conference on Computer Vision and Pattern Recognition* (pp. 1430–1437). https://doi.org/10.1109/CVPR.2013.188

[38] Liu, C., & Gu, J. (2014). Discriminative illumination: Per-pixel classification of raw materials based on optimal projections of spectral BRDF. *IEEE Transactions on Pattern Analysis and Machine Intelligence*, *36*(1), 86–98. https://doi.org/10.1109/TPAMI.2013.110

[39] Jehle, M., Sommer, C., & Jähne, B. (2010). Learning of optimal illumination for material classification. *Lecture Notes in Computer Science*, 6376 LNCS (September), 563–572. https://doi.org/10.1007/978-3-642-15986-2_57

[40] Altman, N. S. (1992). An introduction to kernel and nearest-neighbor nonparametric regression. *American Statistician*, *46*(3), 175–185. https://doi.org/10.1080/00031305.1992.10475879

[41] Marszałek, K., Wolska, N., & Jaglarz, J. (2015). Angle resolved scattering combined with optical profilometry as tools in thin films and surface survey. *Acta Physica Polonica* A, *128*(1), 81–86. https://doi.org/10.12693/APhysPolA.128.81

[42] Mocanu, D. C., & Mocanu, E. (2018). One-shot learning using mixture of variational autoencoders: A generalization learning approach. *ArXiv*, April.

[43] Varmuza, K., Filzmoser, P., Hilchenbach, M., Krüger, H., & Silén, J. (2014). KNN classification - evaluated by repeated double cross validation: Recognition of minerals relevant for comet dust. *Chemometrics and Intelligent Laboratory Systems*, *138*, 64–71. https://doi.org/10.1016/j.chemolab.2014.07.011

[44] Chen, L., Wang, C., Chen, J., Xiang, Z., & Hu, X. (2020). Voice Disorder Identification by using Hilbert-Huang Transform (HHT) and K Nearest Neighbor (KNN). *Journal of Voice*. https://doi.org/10.1016/j.jvoice.2020.03.009

[45] Elgamel, M. S., & Dandoush, A. (2015). A modified Manhattan distance with application for localization algorithms in ad-hoc WSNs. *Ad Hoc Networks*, *33*, 168–189. https://doi.org/10.1016/j.adhoc.2015.05.003

[46] Peiravi, A., & Kheibari, H. T. (2008). A fast algorithm for connectivity graph approximation using modified Manhattan distance in dynamic networks. *Applied Mathematics and Computation*, *201*(1–2), 319–332. https://doi.org/10.1016/j.amc.2007.12.026

[47] Savitzky, A., & Golay, M. J. E. (1964). Smoothing and Differentiation of Data by Simplified Least Squares Procedures. *Analytical Chemistry*. *36*(8): 1627–1639.

[48] Schmid, M., Rath, D., & Diebold, U. (2022). Why and How Savitzky–Golay Filters Should Be Replaced. *ACS Measurement Science Au*, *2*(2), 185–196.

[49] van der Walt, S., Colbert, S. C., & Varoquaux, G. (2011). The NumPy Array: A Structure for Efficient Numerical Computation. *Computing in Science & Engineering*, *13*(2), 22–30. https://doi.org/10.1109/MCSE.2011.37